

Exchange interactions of Yb^{3+} ions in $\text{Yb}_x\text{Y}_{1-x}\text{Ba}_2\text{Cu}_3\text{O}_y$

V. Likodimos and N. Guskos*

Solid State Section, Department of Physics, University of Athens, 157 84 Zografos, Panepistimiopolis, Athens, Greece

M. Wabia and J. Typek

Institute of Physics, Technical University of Szczecin, Al. Piastow 17, 70-310 Szczecin, Poland

(Received 5 November 1997; revised manuscript received 4 June 1998)

The EPR spectrum of Yb^{3+} ions in $\text{Yb}_x\text{Y}_{1-x}\text{Ba}_2\text{Cu}_3\text{O}_y$ ($x=1.0, 0.5$) is studied as a function of temperature. In the oxygen-deficient superconducting phase, the Yb^{3+} EPR spectrum comprises a broad EPR line described by a rhombic g tensor and anisotropic linewidths along the principal axes. Analysis of the EPR linewidth provides an estimate for the effective isotropic exchange interaction, $J/k_B \approx 0.3$ K, between Yb^{3+} ions, indicating that the magnetic ordering of the Yb^{3+} sublattice is determined by the interplay between the short-range exchange interactions and the long-range dipole-dipole interactions. [S0163-1829(98)06737-X]

One of the interesting features of the $R\text{Ba}_2\text{Cu}_3\text{O}_y$ (R rare earth) compounds is the coexistence of superconductivity with the antiferromagnetic (AFM) ordering of the rare-earth sublattice,¹ which is believed to be the result of the relative isolation of R^{3+} ions from the CuO_2 superconducting layers. Theoretical work has shown that the dipole-dipole coupling of R^{3+} ions is the dominant long-range interaction (Ref. 2) which, however, only partly accounts for the observed AFM ordering of the R layers, implying the presence of significant exchange interactions.³ EPR spectroscopy has been employed to elucidate the origin of the magnetic coupling of Gd^{3+} ions in $\text{Gd}_x\text{Y}_{1-x}\text{Ba}_2\text{Cu}_3\text{O}_y$.⁴⁻¹¹ It was established that the EPR linewidth for high Gd concentrations is mainly determined by the dipole-dipole and exchange interactions (Refs. 6-8) and to a lesser extent by the coupling with the charge carriers.⁹⁻¹¹

In the present paper, an EPR study on $\text{Yb}_x\text{Y}_{1-x}\text{Ba}_2\text{Cu}_3\text{O}_y$ ($x=1.0, 0.5$) compounds has been carried out in order to trace the exchange interactions of Yb^{3+} ions. Polycrystalline samples of $\text{YbBa}_2\text{Cu}_3\text{O}_y$ and $\text{Y}_{0.5}\text{Yb}_{0.5}\text{Ba}_2\text{Cu}_3\text{O}_y$ ($y \approx 0.95$, $T_c \approx 93$ K) (samples A) have been prepared by the solid-state method.¹² Part of the samples has been subjected to annealing in He at 850 °C for 4 h, followed by fast quenching at room temperature in He atmosphere (samples B). The latter samples as monitored by the nonresonant microwave absorption (MWA) signal retained part of their superconducting properties. Further suppression of superconductivity was obtained by increasing the annealing temperature to 900 °C and the annealing time to 24 h (samples C). Samples were characterized with powder x-ray diffraction using a D5000 Siemens diffractometer with $\text{Cu } K\alpha$ radiation, while temperature-dependent EPR measurements were carried out using an X-band Bruker 200D spectrometer with an Oxford flow cryostat.

EPR measurements carried on samples A in the temperature range $T=4-100$ K, have not given any appreciable sign of the Yb^{3+} EPR spectrum mainly due to the interference of the intense MWA signal. The latter absorption inherent to all high- T_c superconductors at $T < T_c$ produces a highly nonlinear baseline which severely distorts the EPR spectra. Subsequently, EPR measurements were carried out on samples B

where the MWA signal has been substantially reduced, at least in the higher temperature range [Figs. 1(a) and 1(b)]. The EPR spectra for both samples B comprise the contribution of an intense, almost "isotropic" EPR line in the $g \approx 2$ region, more pronounced at low temperatures ($T=4-30$ K), which can be related to the EPR signal from localized clusters in oxygen-deficient $R123$ compounds,¹³ a weak anisotropic Cu^{2+} EPR spectrum and an intense broad EPR signal at $g_{\text{eff}} \approx 3.42$ overlapping with MWA at low temperatures, which results from the EPR absorption of Yb^{3+} ions.

According to the crystal-field interaction of Yb^{3+} ($4f^{13}$) in $\text{YbBa}_2\text{Cu}_3\text{O}_7$ (Ref. 14) that splits the eightfold degenerate $^2F_{7/2}$ ground term in four Γ_5 Kramers doublets, the EPR spectrum of the ground doublet is described by a rhombic spin Hamiltonian (D_{2h}) for effective spin $S=1/2$ with principal g values $g_x=3.44$, $g_y=3.47$, $g_z=3.36$, where the x, y, z axes correspond to the a, b, c crystallographic axes. The effective average value $g_{\text{eff}}=(g_x+g_y+g_z)/3=3.423$ is very close to the experimental g_{eff} value. The line shape of the Yb^{3+} EPR signal is close to the full Lorentzian which takes into account both absorptions at $+H_r$ and $-H_r$ caused by

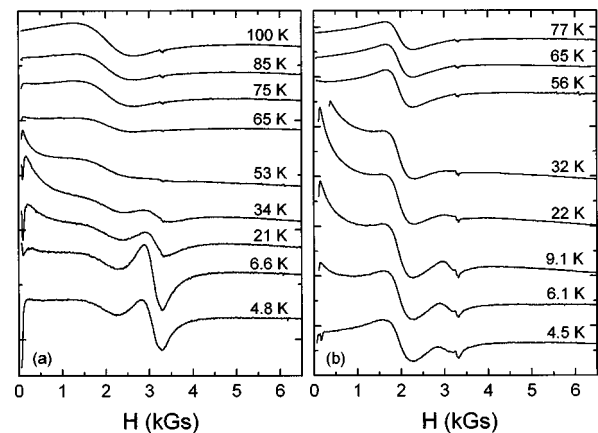


FIG. 1. Temperature dependence of the X-band EPR spectra for $\text{Yb}_x\text{Y}_{1-x}\text{Ba}_2\text{Cu}_3\text{O}_y$ samples B (a) $x=1.0$, (b) $x=0.5$. The spectra are in arbitrary scale.

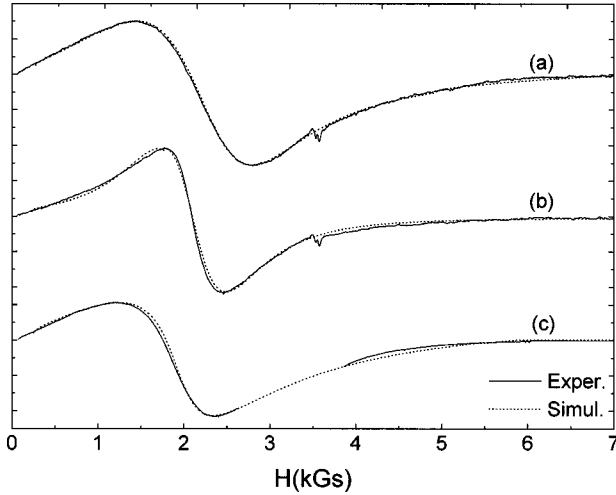


FIG. 2. Simulation of the X-band Yb^{3+} EPR spectra in $\text{Yb}_x\text{Y}_{1-x}\text{Ba}_2\text{Cu}_3\text{O}_y$, (a) $x=1.0$, sample *B*, $T=100$ K, (b) $x=0.5$, sample *B*, $T=77$ K, (c) $x=0.5$, sample *C*, $T=10$ K.

the two oppositely rotating components of the linearly polarized rf field. However, the EPR spectrum cannot be accurately fitted with single Lorentzian line shape. Powder simulation has been performed using the MONOQF program (Ref. 15) for spin $S=1/2$, allowing for the two odd isotopes of Yb^{3+} (^{171}Yb , $I=1/2$, 14.31%, ^{173}Yb , $I=5/2$, 16.13%), at high temperatures where the interference of MWA is suppressed. The results of the simulation for samples *B* after correcting for a superimposed sloping baseline are shown in Fig. 2, while the corresponding g values and linewidths are shown in Table I. The hyperfine parameters not included in Table I, have been kept constant to the values predicted by $g_i/A_i = g_J/A_J$ ($i=a,b,c$), with g_J and A_J being the Lande g factor and the hyperfine coupling constant for the $^2\text{F}_{7/2}$ ground term, due to the small J mixing of the different energy terms for Yb^{3+} ions.

The linewidth ΔH for both samples *B* remained constant within experimental error (± 50 Gs), at least in the range of $T=60$ – 100 K, since at lower temperatures the spectrum is severely masked by the MWA signal. The absence of thermal broadening of ΔH indicates that Korringa-like relaxation of the localized Yb moments through the coupling with charge carriers is weak, complying with Mössbauer results which showed low conduction-electron density at the Yb site.¹⁶ Considering the Korringa thermal rates reported for Gd^{3+} EPR spectrum in Y123 and Eu123 compounds, $\Delta H_K/T \approx 0.5$ G/K (Refs. 9–11), we derive a thermal broadening of ≈ 50 Gs up to $T=100$ K, which is comparable to

the experimental error in the measurement of ΔH . Previous Mössbauer and EPR studies on Yb-doped Y123 samples,^{16,17} showed that spin-lattice relaxation lead to linewidths varying nonlinearly (Orbach and/or Raman processes) from ≈ 500 to ≈ 800 MHz in the range of $T=50$ – 90 K, which are considerably smaller than the experimental ΔH values. Therefore, it is plausible to consider that the anisotropic Yb^{3+} EPR linewidth in $\text{Yb}_x\text{Y}_{1-x}\text{Ba}_2\text{Cu}_3\text{O}_y$ ($x=1.0, 0.5$) compounds is determined by Yb^{3+} spin-spin coupling.

In the case of samples *C*, the MWA signal was drastically reduced indicating the suppression of superconductivity, while the intensity of the copper EPR spectra was greatly enhanced in comparison with that of the Yb^{3+} EPR spectrum. An approximate simulation of the Yb^{3+} EPR spectrum due to its superposition with the intense Cu^{2+} EPR signal, in $\text{Yb}_{0.5}\text{Y}_{0.5}\text{Ba}_2\text{Cu}_3\text{O}_y$ sample *C* (Fig. 2), indicates the presence of considerable g shift and a substantial increase of ΔH (Table I) complying with previous EPR and Mössbauer results which have been interpreted in terms of a fluctuating molecular field caused by the interaction of Yb^{3+} with the adjacent CuO_2 planes.^{16,17}

Were Yb^{3+} ions coupled only by the dipole-dipole interaction, the line shape would be Gaussian and the EPR linewidth would be determined from the value of the secular second moment $M_2^{(0)}$.¹⁸ Applying the arguments of Kittel and Abrahams (Ref. 19) for the concentration dependence of the lattice sums involved in the second moment, the secular $M_2^{(0)}$ in the high-temperature approximation ($k_B T \gg h\nu$) has been calculated as a function of Yb^{3+} concentration (x). Taking into account the rhombic g tensor, $M_2^{(0)}$ along the principal axes is a function of six lattice sums, independent on the orientation of the magnetic field, which have been numerically calculated within a $6a \times 6b$ rectangular block with lattice parameters $a=3.800$ Å and $b=3.872$ Å.²⁰ Due to the relatively large distance between the *R* layers along the *c* axis ($c \sim 3a$) in the *R*123 structure, in the preceding derivation we have considered only Yb^{3+} ions lying in the same *ab* plane with $a \neq b$, which makes some of the elements of the dipolar tensor zero. The half width at half height for a Gaussian spectral line along the principal directions, in frequency units, is expressed as $\Delta H_i = \sqrt{2 \ln 2} \sqrt{M_{2i}^{(0)}}$, ($i=a,b,c$) which result in the dipolar EPR widths ΔH_d listed in Table I. These values are considerably larger than the EPR linewidths for samples *B*, attesting that exchange narrowing is effective.^{18,21}

In this case, we introduce $H_{\text{ex}} = \sum_{j,k} J_{jk} S_j \cdot S_k$ to describe the exchange interaction of Yb^{3+} spins with J_{jk} being the isotropic exchange coupling constant between two nearest-

TABLE I. The g values and linewidths along the principal a,b,c axes derived from the simulation of the Yb^{3+} EPR spectra in $\text{Yb}_x\text{Y}_{1-x}\text{Ba}_2\text{Cu}_3\text{O}_y$. The calculated dipolar EPR linewidths are also included.

	Simulated						Dipolar			
	g_a	g_b	g_c	ΔH_a (GHz)	ΔH_b (GHz)	ΔH_c (GHz)	T (K)	ΔH_a (GHz)	ΔH_b (GHz)	ΔH_c (GHz)
$\text{YbBa}_2\text{Cu}_3\text{O}_y$ (<i>B</i>)	3.45(5)	3.85(5)	3.10(5)	6.5(1)	6.7(1)	2.8(1)	100	8.30	8.84	4.77
$\text{Yb}_{0.5}\text{Y}_{0.5}\text{Ba}_2\text{Cu}_3\text{O}_y$ (<i>B</i>)	3.50(6)	3.90(6)	3.20(6)	3.9(1)	4.2(1)	1.8(1)	77	5.88	6.25	3.38
$\text{Yb}_{0.5}\text{Y}_{0.5}\text{Ba}_2\text{Cu}_3\text{O}_y$ (<i>C</i>)	3.7(1)	3.9(1)	3.5(1)	9.0(2)	7.5(2)	3.0(2)	10	5.88	6.25	3.38

neighbor (NN) effective spins j and k . It should be noted that the assumption of isotropic exchange between the real Yb^{3+} spins is arguable, due to the orbital contribution in the rare-earth ground state which introduces nonzero anisotropic contributions in the exchange integral.²² Assuming that $\nu_0 \gg \nu_{\text{ex}}$ (adiabatic approximation), where ν_{ex} is the cutoff (exchange) frequency which corresponds to the rate at which the exchange interaction modulates the dipolar perturbation and ν_0 is the resonance frequency, the half width at half height for a Lorentzian line is given by $\Delta H = (\pi/2\sqrt{3})(M_2/\mu)^{1/2} = (\pi/2)(M_2/\nu_{\text{ex}})$, where M_4 is the fourth moment of the resonance line and $\mu = M_4/M_2^2$ with $\mu \gg 3$. Using the values of ΔH_i determined from the simulation of the Yb^{3+} EPR spectrum for $x=1.0$ (Table I) and the derived $M_{2i}^{(0)}$ ($i = a, b, c$), we obtain the values of 11 860, 12 650, and 9930 MHz for ν_{ex} along the a, b, c axes. These values do not comply with the condition $\nu_0 \gg \nu_{\text{ex}}$ ($\nu_0 = 9430$ MHz), indicating that the adiabatic condition is not fulfilled. In the case of $\nu_{\text{ex}} \approx \nu_0$ a frequency-dependent linewidth is expected.²³ Following Kubo and Tomita (Ref. 23) we may approximate the frequency dependence of the second moment by $M_2 \approx M_2^{(0)} + M_2^{(1)} \exp(-\nu_0^2/2\nu_{\text{ex}}^2) + M_2^{(2)} \exp(-2\nu_0^2/\nu_{\text{ex}}^2)$, which for $\nu_{\text{ex}} \gg \nu_0$ reaches the total second moment $M_2^{(f)} = M_2^{(0)} + M_2^{(1)} + M_2^{(2)}$. Subsequently, the full $M_2^{(f)}$ which is a function of seven lattice sums, has been calculated including the nonsecular terms of the dipolar tensor.²⁴ Then, using the values of the contributions $M_2^{(0)}$, $M_2^{(1)}$, and $M_2^{(2)}$ in M_2 and the ν_{ex} values determined from the experimental linewidths for $x=1.0$, we approximate the second moment along the principal axes as $M_{2a} \approx 1.2M_{2a}^{(0)}$, $M_{2b} \approx 1.2M_{2b}^{(0)}$ and $M_{2c} \approx 1.6M_{2c}^{(0)}$.

The secular $M_4^{(0)}$ ($k_B T \gg h\nu$) for spin $S=1/2$,¹⁸ reduces to

$$M_4^{(0)} = \frac{x^2}{16h^4} \sum_{k,l \neq j} [3B_{jk}^2 B_{jl}^2 + 2A_{jk}^2 (B_{jl} - B_{kl})^2 + 2A_{jk} A_{kl} (B_{jl} - B_{jk})(B_{jl} - B_{kl}) + 2A_{jk} B_{jk} (B_{jl} - B_{kl})^2] + \frac{x}{8h^4} \sum_k B_{jk}^4, \quad (1)$$

where $A_{jk} = J_{jk} - \frac{1}{2}D'_{jzkz}$ and $B_{jk} = \frac{3}{2}D'_{jzkz}$ with $D'_{jzkz} = (2D_{jzkz} - D_{jxkx} - D_{jyky})/3$ and $D_{j\mu k\nu}(\mu, \nu = x, y, z)$ being the elements of the dipolar tensor in the Zeeman representation. In Eq. (1) the implicated lattice sums over randomly filled sites are converted to sums over all sites, while k, l are taken as summation indices and j labels a fixed lattice with the restriction that $j \neq k \neq l$. Taking $J_{jk} = J$, if j and k are NN ions along the a or b axes, the computation of $M_4^{(0)}$ which can be separated in two parts, the purely dipolar contribution $M_{4,d}^{(0)}$ and that comprising the exchange interaction $M_{4,\text{ex}}^{(0)}$, involves a large number of summations. The latter have been carried out assuming for simplicity a square lattice with lattice constant $(a+b)/2 = 3.836 \text{ \AA}$, the calculation being performed for a radius of seven lattice constants, and axial g tensor with $g_{\perp} = (g_a + g_b)/2$ and $g_{\parallel} = g_c$. Simplifications such as the negligence of the linear terms in J_{jk} or that of the dipolar contribution to A_{jk} ,¹⁸ have not been made since the latter terms give a small but not negligible contribution in

TABLE II. Exchange coupling constants J of Yb^{3+} ions in $\text{Yb}_x\text{Y}_{1-x}\text{Ba}_2\text{Cu}_3\text{O}_y$ samples B for magnetic field along the a and c axes.

x	$H \parallel a$			$H \parallel c$		
	μ_a	$\mu_{\text{ex}}^{(a)}$	J (μeV)	μ_c	$\mu_{\text{ex}}^{(c)}$	J (μeV)
1.0	4.07	1.59	25.7	7.13	4.83	26.1
0.5	4.93	1.78	27.1	7.90	5.23	27.2

$M_4^{(0)}$. Assuming the same frequency dependence for M_2 and M_4 ,²⁵ we derive the ratio μ parallel to the a and c axes,

$$\mu_d^{(a)} = 1.826 + \frac{0.66}{x}, \quad \mu_d^{(c)} = 1.939 + \frac{0.364}{x},$$

$$\mu_{\text{ex}}^{(a)} = (48.8J^2 - 45\,490J)(10^{-9} \text{ MHz}^2), \quad (2)$$

$$\mu_{\text{ex}}^{(c)} = (133J^2 - 78\,000J)(10^{-9} \text{ MHz}^2),$$

where $\mu_d = M_{4,d}/M_{2,d}^2$ and $\mu_{\text{ex}} = M_{4,\text{ex}}/M_{2,d}^2$. From Eqs. (2) the values of μ turn out to be not much larger than three indicating that the condition $\mu \gg 3$ required for Lorentzian line shape is not fully justified. In this case, we make use of the formula, previously applied in the analysis of the Gd^{3+} EPR linewidth,¹¹ covering the transition from the Gaussian to Lorentzian line shape according to the value of μ ,

$$\Delta H = \sqrt{\frac{\pi}{2}} \left(\frac{M_2}{\mu - 1.87} \right)^{1/2}.$$

Substituting in the previous relation the simulated ΔH values for samples B (Table I), μ_a and μ_c are determined. Then, substituting in Eqs. (2) the latter values for μ which is defined as $\mu = \mu_d + \mu_{\text{ex}}$, the positive roots corresponding to the AFM interaction according to the present notation of H_{ex} , provide the exchange interaction constants (Table II). The values of J thus derived from the two orientations of the magnetic field and for the two Yb concentrations are consistent with each other, though a small increase of J is derived for $x=0.5$, which might be associated with a slight contribution of spin-lattice relaxation in the corresponding EPR linewidth.

Although, there have not been any reports on the magnitude of the exchange coupling for Yb^{3+} ions in $\text{Yb}123$, the value of $J/k_B \approx 0.3 \text{ K}$ is reasonable regarding the Néel temperature $T_N \approx 0.33 \text{ K}$ reported for the AFM ordered Yb^{3+} sublattice.^{26,27} In a previous theoretical work the low-temperature ordered states of the $R123$ compounds have been calculated, taking into account the dipole-dipole and exchange interactions of R^{3+} ions.² Using the exchange coupling constant derived for Yb^{3+} ions in the present work, we find that the dipolar contribution for the predicted lowest-lying ordering configurations with the magnetic moment along the b axis, becomes comparable to the exchange contribution. Moreover, neither of the lowest-lying energies predicted for the orthorhombically distorted tetragonal $R123$

structure corresponds to the experimental configuration, $q(6y)$, of the Yb^{3+} sublattice. The latter discrepancy may be due to the exchange contribution which turns out to be comparable to the dipolar one.

In conclusion, the present EPR study of $\text{Yb}_x\text{Y}_{1-x}\text{Ba}_2\text{Cu}_3\text{O}_y$ ($x=1.0, 0.5$) compounds provides evidence for the presence of exchange coupling between NN Yb^{3+} ions with an effective isotropic exchange constant of $J/k_B \approx 0.3$ K. Accordingly, it is deduced that the low-

temperature ordered state of Yb^{3+} comprises a substantial exchange contribution comparable to the dipolar one, indicating that the magnetic ordering of the Yb^{3+} sublattice is determined by the interplay between the short-range exchange and the long-range dipole-dipole interactions.

We would like to thank Professor J. R. Pilbrow for providing us with the MONOQF simulation program and Dr. V. Petrouleas for arranging the EPR measurements.

*Author to whom correspondence should be addressed: Solid State Section, Department of Physics, University of Athens, 157 84 Zografos, Panepistimiopolis, Athens, Greece; Fax (+301) 72 57 689; Electronic address: ngouskos@atlas.uoa.gr

¹J. W. Lynn, *J. Alloys Compd.* **181**, 419 (1992).

²S. K. Misra and J. Felsteiner, *Phys. Rev. B* **46**, 11 033 (1992).

³K. De'Bell and J. P. Whitehead, *J. Phys.: Condens. Matter* **3**, 2431 (1990); A. B. Mac Isaak, J. P. Whitehead, K. DeBell, and K. S. Narayanan, *Phys. Rev. B* **46**, 6387 (1992).

⁴M. T. Causa, C. Fainstein, G. Nieva, R. Sanchez, L. B. Steren, M. Tovar, R. Zysler, D. C. Vier, S. Schultz, S. B. Oseroff, Z. Fisk, and J. L. Smith, *Phys. Rev. B* **38**, 257 (1988).

⁵D. Shaltiel, S. E. Barnes, H. Bill, M. Francois, H. Hagemann, J. Jegondaz, D. Lovy, P. Monod, M. Peter, A. Revcolevschi, W. Sadowski, and E. Walker, *Physica C* **161**, 13 (1989).

⁶F. Nakamura, Y. Ochiai, H. Shimizu, and Y. Narahara, *Phys. Rev. B* **42**, 2558 (1990).

⁷A. Deville, L. Bejjit, B. Gaillard, J. P. Sorbier, O. Monnereau, H. Noel, and M. Potel, *Phys. Rev. B* **47**, 2840 (1993).

⁸C. Filip, C. Kessler, F. Balibanu, P. Kleeman, A. Darabont, L. V. Giurgiu, and M. Mehring, *Physica B* **222**, 16 (1996).

⁹A. Janossy, J. R. Cooper, L.-C. Brunel, and A. Carrington, *Phys. Rev. B* **50**, 3442 (1994).

¹⁰D. Shaltiel, C. Noble, J. Pilbrow, D. Hutton, and E. Walker, *Phys. Rev. B* **53**, 12 430 (1996).

¹¹C. Kessler, M. Mehring, P. Castellaz, G. Borodi, C. Filip, A. Darabont, and L. V. Giurgiu, *Physica B* **229**, 113 (1997).

¹²Y. K. Du, G. C. Che, S. L. Jia, and Z. X. Zhao, *J. Solid State Chem.* **112**, 406 (1994).

¹³V. Likodimos, N. Guskos, H. Gamari-Seale, A. Koufoudakis, M. Wabia, J. Typek, and H. Fuks, *Phys. Rev. B* **54**, 12 342 (1996).

¹⁴M. Guillaume, P. Allenspach, J. Mesot, U. Staub, A. Furrer, R. Osborn, A. D. Taylor, F. Stucki, and P. Unternahrer, *Solid State Commun.* **81**, 999 (1992).

¹⁵J. R. Pilbrow, *Transition Ion Electron Paramagnetic Resonance* (Clarendon, Oxford, 1990).

¹⁶J. A. Hodges, P. Bonville, P. Imbert, and G. Jehanno, *Physica C* **184**, 259 (1991); J. A. Hodges, P. Bonville, P. Imbert, G. Jehanno, and P. Debray, *ibid.* **184**, 270 (1991).

¹⁷I. N. Kurkin, I. Kh. Salikhov, L. L. Sedov, M. A. Teplov, and R. Sh. Zhdanov, *JETP* **76**, 657 (1993).

¹⁸J. H. Van Vleck, *Phys. Rev.* **74**, 1168 (1948).

¹⁹C. Kittel and E. Abrahams, *Phys. Rev.* **90**, 238 (1953).

²⁰M. Guillaume, P. Allenspach, W. Henggeler, J. Mesot, B. Roessli, U. Staub, P. Fischer, A. Furrer, and V. Trounov, *J. Phys.: Condens. Matter* **6**, 7963 (1994).

²¹P. W. Anderson and P. R. Weiss, *Rev. Mod. Phys.* **25**, 269 (1953).

²²J. M. Baker, *Rep. Prog. Phys.* **34**, 109 (1971).

²³R. Kubo and K. Tomita, *J. Phys. Soc. Jpn.* **9**, 888 (1954).

²⁴Z. G. Soos, K. T. McGregor, T. T. P. Cheung, and A. J. Silverstein, *Phys. Rev. B* **16**, 3036 (1977).

²⁵J. E. Gulley, D. Hone, D. J. Scalapino, and B. G. Silbernagel, *Phys. Rev. B* **1**, 1020 (1970).

²⁶J. A. Hodges, P. Imbert, and G. Jehanno, *Solid State Commun.* **64**, 1209 (1987).

²⁷B. Roessli, P. Allenspach, P. Fischer, J. Mesot, U. Staub, H. Maletta, P. Bruesch, C. Ritter, and A. W. Hewat, *Physica B* **180&181**, 396 (1992).